Chapter | nine

Rotation-Translation Coupling

Earliest morning, switching all the tracks
that cross the sky from cinder star to star,
coupling the ends of streets
to trains of light.

Elizabeth Bishop (1911–1979)

Thus far, we have discussed point-mass models for relative spacecraft translational motion, including nonlinear modeling in the Cartesian LVLH frame, discussed in Chapter 4, linear models, described in Chapter 5, and orbital-elements-based modeling, elaborated upon in Chapters 6–8. In other words, we focused on three degrees of freedom (DOF) only. Obviously, designing a space mission that consists of several space vehicles requires modeling the relative rotational motion in addition to the relative translation, i.e., six-degrees-of-freedom models.

It has been well-known that there exists an analogy between orbital dynamics and rigid-body dynamics [129]. We have pointed out this analogy in Sections 2.4, 7.1 and 7.2, where tools from attitude parameterizations, namely Euler parameters, were used for modeling relative translational dynamics. However, models for the relative motion of six-DOF spacecraft have gained attention in the literature only in recent years. Among the first to model the spacecraft relative angular velocity in the framework of spacecraft formation flying were Pan and Kapila [158], who addressed the coupled translational and rotational dynamics of two spacecraft. By defining two body-fixed reference frames, one attached to the chief and the other attached to the deputy, Pan and Kapila proposed using a two-part relative motion model: One that accounts for the relative translational dynamics of the body-fixed coordinate frame origins, and another that captures the relative attitude dynamics of the two body-fixed frames. A similar modeling approach was used for relative motion estimation [159]. In addition, tensorial equations of motion for a formation consisting of N spacecraft, each modeled as a rigid body, were derived [160], and

Spacecraft Formation Flying; ISBN: 9780750685337

coordination architectures relying on six-DOF models were developed for spacecraft interferometry applications [161].

In general, rigid-body dynamics can be represented as translation of the center-of-mass (CM) and rotation about the CM [162]. Thus, spacecraft relative motion must be composed by combining the relative translational and rotational dynamics of arbitrary points on the spacecraft. Whenever one of these points, termed *feature points*, does not coincide with the spacecraft's CM, a kinematic coupling between the rotational and translational dynamics of these points occurs.

The purpose of this chapter is to model the kinematic coupling effect and to show that this effect is key for high-precision modeling of tight formation flying, rendezvous, and docking. This effect, originally pointed out by Segal and Gurfil [163], is also important in vision-based relative attitude and position control, where arbitrary feature points on a target vehicle are tracked. Given two rigid-body spacecraft, the model presented herein is formulated in a general manner that describes the motion between any two arbitrary points on the spacecraft. Hence, the relative translational motion between feature points on different satellites is a function of their orbital and attitude motions.

We will also provide a CW-like approximation of the relative motion that includes the kinematic coupling effect. This approximation is aimed at alleviating an apparent contradiction in linearized relative motion theories: To obtain linear equations of motion, the spacecraft are assumed to operate in close proximity. However, if the spacecraft are close to each other (e.g. rendezvous), then they can no longer be treated as point masses, since the spacecraft shape and size affects the relative translation between off-CM points. This effect is accentuated as the distances between spacecraft decrease.

9.1 RELATIVE DYNAMICS

As in previous chapters, we consider two rigid-body spacecraft orbiting the Earth: One of them is a chief and the other is a deputy. We will use the standard coordinate systems introduced in Chapter 2, namely $\mathscr{I}$, the ECI frame, $\mathscr{L}_0$, the chief-fixed LVLH frame, and $\mathscr{L}_1$, the deputy-fixed LVLH frame. In addition, we will assume that the orbital frames $\mathscr{L}_0$ and $\mathscr{L}_1$ coincide with the body-fixed frames of the chief and deputy spacecraft, respectively.[1] In Chapter 4, we developed the equations of relative orbital motion (4.14)–(4.16). In the absence of orbital perturbations, $\dot{\theta}_0 = \dot{f}_0$, so Eqs. (4.14)–(4.16) become

$$\ddot{x} - 2\dot{f}_0\dot{y} - \ddot{f}_0 y - \dot{f}_0^2 x = -\frac{\mu(r_0 + x)}{[(r_0 + x)^2 + y^2 + z^2]^{\frac{3}{2}}} + \frac{\mu}{r_0^2} \tag{9.1a}$$

$$\ddot{y} + 2\dot{f}_0\dot{x} + \ddot{f}_0 x - \dot{f}_0^2 y = -\frac{\mu y}{[(r_0 + x)^2 + y^2 + z^2]^{\frac{3}{2}}} \tag{9.1b}$$

[1] In reality, gravity gradient effects can cause attitude oscillations. For elliptic orbits, there is an inherent orbit and attitude coupling. For spin-stabilized satellites with inertial pointing, the body axes and the LVLH axes are quite different. We are neglecting these effects here, assuming that the attitude controller is maintaining LVLH pointing.

$$\ddot{z} = -\frac{\mu z}{[(r_0 + x)^2 + y^2 + z^2]^{\frac{3}{2}}} \tag{9.1c}$$

We define the rotational angular velocity of the deputy relative to the chief, $\delta\boldsymbol{\omega} \in \mathbb{R}^3$ as

$$\delta\boldsymbol{\omega} \triangleq \boldsymbol{\omega}_1 - \boldsymbol{\omega}_0 \tag{9.2}$$

where $\boldsymbol{\omega}_0$ and $\boldsymbol{\omega}_1$ are the respective angular velocities of the deputy and the chief, respectively, in some given reference frame.

The relative attitude can be parameterized using a rotation matrix $D \in \mathrm{SO}(3)$, which transforms a vector from the body-fixed frame $\mathscr{L}_1$ to the body-fixed frame $\mathscr{L}_0$. The relative attitude will be parameterized using the relative Euler parameters, which we defined by Eqs. (2.52)–(2.54), and used in Section 7.2. Recall that [164]

$$\delta\beta_1 \triangleq e_1 \sin\frac{\wp}{2}, \delta\beta_2 \triangleq e_2 \sin\frac{\wp}{2}, \delta\beta_3 \triangleq e_3 \sin\frac{\wp}{2}, \delta\beta_0 \triangleq \cos\frac{\wp}{2} \tag{9.3}$$

subject to the constraint

$$\delta\beta_1^2 + \delta\beta_2^2 + \delta\beta_3^2 + \delta\beta_0^2 = 1 \tag{9.4}$$

In Eq. (9.3), $[e_1, e_2, e_3]^T$ constitutes a vector along the axis of rotation, and $\wp$ is the angle of the rotation from $\mathscr{L}_0$ to $\mathscr{L}_1$. As we mentioned in Sections 7.1 and 7.2, the Euler parameters form a quaternion, $\delta\boldsymbol{\beta} = [\delta\beta_0, \delta\beta_1, \delta\beta_2, \delta\beta_3]^T$, where $[\delta\beta_1, \delta\beta_2, \delta\beta_3]^T$ is the vector part and $\delta\beta_0$ is the scalar part. In the subsequent discussion, we will drop the δ symbol before the relative quantities for the ease of notation; we thus write $\delta\beta_i \equiv \beta_i$ and $\delta\boldsymbol{\omega} \equiv \boldsymbol{\omega}$.

The rotation matrix, D, can be expressed in terms of the quaternion as

$$D(\boldsymbol{\beta}) = \begin{bmatrix} \beta_1^2 - \beta_2^2 - \beta_3^2 + \beta_0^2 & 2(\beta_1\beta_2 - \beta_3\beta_0) & 2(\beta_1\beta_3 + \beta_2\beta_0) \\ 2(\beta_1\beta_2 + \beta_3\beta_0) & -\beta_1^2 + \beta_2^2 - \beta_3^2 + \beta_0^2 & 2(\beta_2\beta_3 - \beta_1\beta_0) \\ 2(\beta_1\beta_3 - \beta_2\beta_0) & 2(\beta_2\beta_3 + \beta_1\beta_0) & -\beta_1^2 - \beta_2^2 + \beta_3^2 + \beta_0^2 \end{bmatrix} \tag{9.5}$$

Using $D(\boldsymbol{\beta})$, the relative angular velocity vector, $\boldsymbol{\omega}$, can be calculated in the body-fixed frames $\mathscr{L}_0$ and $\mathscr{L}_1$, respectively, as follows:

$$[\boldsymbol{\omega}]_{\mathscr{L}_0} = D(\boldsymbol{\beta})[\boldsymbol{\omega}_1]_{\mathscr{L}_1} - [\boldsymbol{\omega}_0]_{\mathscr{L}_0} \tag{9.6}$$

Utilizing $\boldsymbol{\omega}$ and $\boldsymbol{\beta}$, the attitude kinematics of the deputy relative to the chief can be described using the quaternion kinematic equations of motion

$$\dot{\boldsymbol{\beta}} = \frac{1}{2} Q(\boldsymbol{\beta})[\boldsymbol{\omega}]_{\mathscr{L}_1} \tag{9.7}$$

where

$$Q(\boldsymbol{\beta}) = \begin{bmatrix} -\beta_1 & -\beta_2 & -\beta_3 \\ \beta_0 & -\beta_3 & \beta_2 \\ \beta_3 & \beta_0 & -\beta_1 \\ -\beta_2 & \beta_1 & \beta_0 \end{bmatrix} \tag{9.8}$$

The attitude dynamics of the deputy relative to the chief, expressed in $\mathscr{L}_0$, will now be derived according to the guidelines of Ref. [158]. First, a differentiation of Eq. (9.2) with respect to the inertial frame leads to

$$\frac{\mathrm{d}^{\mathscr{I}}\boldsymbol{\omega}}{\mathrm{d}t} = \frac{\mathrm{d}^{\mathscr{I}}\boldsymbol{\omega}_1}{\mathrm{d}t} - \frac{\mathrm{d}^{\mathscr{I}}\boldsymbol{\omega}_0}{\mathrm{d}t} \tag{9.9}$$

Expressing Eq. (9.9) in the body-fixed frame $\mathscr{L}_0$ yields

$$\left(\frac{\mathrm{d}^{\mathscr{I}}\boldsymbol{\omega}}{\mathrm{d}t}\right)_{\mathscr{L}_0} = D(\boldsymbol{\beta})\left(\frac{\mathrm{d}^{\mathscr{I}}\boldsymbol{\omega}_1}{\mathrm{d}t}\right)_{\mathscr{L}_1} - \left(\frac{\mathrm{d}^{\mathscr{I}}\boldsymbol{\omega}_0}{\mathrm{d}t}\right)_{\mathscr{L}_0} \tag{9.10}$$

On the other hand,

$$\frac{\mathrm{d}^{\mathscr{I}}\boldsymbol{\omega}}{\mathrm{d}t} = \left(\frac{\mathrm{d}\boldsymbol{\omega}}{\mathrm{d}t}\right)_{\mathscr{L}_0} + \boldsymbol{\omega}_0 \times \boldsymbol{\omega} \tag{9.11}$$

Expressing Eq. (9.11) in $\mathscr{L}_0$ provides us with the expression

$$\left(\frac{\mathrm{d}^{\mathscr{I}}\boldsymbol{\omega}}{\mathrm{d}t}\right)_{\mathscr{L}_0} = \left(\frac{\mathrm{d}\boldsymbol{\omega}}{\mathrm{d}t}\right)_{\mathscr{L}_0} + [\boldsymbol{\omega}_0]_{\mathscr{L}_0} \times [\boldsymbol{\omega}]_{\mathscr{L}_0} \tag{9.12}$$

Comparing Eq. (9.10) to Eq. (9.12) yields

$$\left(\frac{\mathrm{d}\boldsymbol{\omega}}{\mathrm{d}t}\right)_{\mathscr{L}_0} = D(\boldsymbol{\beta})\left(\frac{\mathrm{d}^{\mathscr{I}}\boldsymbol{\omega}_1}{\mathrm{d}t}\right)_{\mathscr{L}_1} - \left(\frac{\mathrm{d}^{\mathscr{I}}\boldsymbol{\omega}_0}{\mathrm{d}t}\right)_{\mathscr{L}_0} - [\boldsymbol{\omega}_0]_{\mathscr{L}_0} \times [\boldsymbol{\omega}]_{\mathscr{L}_0} \tag{9.13}$$

The differentiation of the angular velocity in a fixed frame or in a body frame gives the same result. Using this fact and multiplying Eq. (9.13) by the inertia tensor of the chief, $\mathbb{I}_0 \in \mathbb{R}^{3\times 3}$, gives

$$\begin{aligned} \mathbb{I}_0\left(\frac{\mathrm{d}^{\mathscr{L}_0}\boldsymbol{\omega}}{\mathrm{d}t}\right)_{\mathscr{L}_0} = {} & \mathbb{I}_0 D(\boldsymbol{\beta})\left(\frac{\mathrm{d}^{\mathscr{L}_1}\boldsymbol{\omega}_1}{\mathrm{d}t}\right)_{\mathscr{L}_1} - \mathbb{I}_0\left(\frac{\mathrm{d}^{\mathscr{L}_0}\boldsymbol{\omega}_0}{\mathrm{d}t}\right)_{\mathscr{L}_0} \\ & - \mathbb{I}_0\,[\boldsymbol{\omega}_0]_{\mathscr{L}_0} \times [\boldsymbol{\omega}]_{\mathscr{L}_0} \end{aligned} \tag{9.14}$$

Eq. (9.14) relates the derivative of the relative angular velocity to the angular velocities rates of the deputy and the chief, thus yielding the relative rotational

dynamic equations. The relative dynamics in terms of $\mathscr{L}_0$-quantities can be obtained by writing

$$\frac{\mathrm{d}\mathbf{H}}{\mathrm{d}t} = \mathbf{N} \tag{9.15}$$

where $\mathbf{H}$ is the total angular momentum and $\mathbf{N}$ is an external torque. Expressing (9.15) in body axes yields

$$\frac{\mathrm{d}^{\mathscr{I}}\mathbf{H}_1}{\mathrm{d}t} = \frac{\mathrm{d}^{\mathscr{L}_1}\mathbf{H}_1}{\mathrm{d}t} + \boldsymbol{\omega}_1 \times \mathbf{H}_1 = \mathbf{N}_1 \tag{9.16}$$

$$\frac{\mathrm{d}^{\mathscr{I}}\mathbf{H}_0}{\mathrm{d}t} = \frac{\mathrm{d}^{\mathscr{L}_0}\mathbf{H}_0}{\mathrm{d}t} + \boldsymbol{\omega}_0 \times \mathbf{H}_0 = \mathbf{N}_0 \tag{9.17}$$

Since $\mathbf{H}_0 = \mathbb{I}_0\boldsymbol{\omega}_0$ and $\mathbf{H}_1 = \mathbb{I}_1\boldsymbol{\omega}_1$, with $\mathbb{I}_1 \in \mathbb{R}^{3\times 3}$ being the inertia tensor of the deputy,

$$\mathbb{I}_1\frac{\mathrm{d}^{\mathscr{I}}\boldsymbol{\omega}_1}{\mathrm{d}t} = \mathbb{I}_1\frac{\mathrm{d}^{\mathscr{L}_1}\boldsymbol{\omega}_1}{\mathrm{d}t} + \boldsymbol{\omega}_1 \times \mathbb{I}_1\boldsymbol{\omega}_1 = \mathbf{N}_1 \tag{9.18}$$

and

$$\mathbb{I}_0\frac{\mathrm{d}^{\mathscr{I}}\boldsymbol{\omega}_0}{\mathrm{d}t} = \mathbb{I}_0\frac{\mathrm{d}^{\mathscr{L}_0}\boldsymbol{\omega}_0}{\mathrm{d}t} + \boldsymbol{\omega}_0 \times \mathbb{I}_0\boldsymbol{\omega}_0 = \mathbf{N}_0 \tag{9.19}$$

where $\mathbf{N_0}$ and $\mathbf{N_1}$ are external torques acting on the chief and deputy, respectively. Now, substituting Eqs. (9.18) and (9.19) into Eq. (9.14) gives

$$\begin{aligned}\mathbb{I}_0\left(\frac{\mathrm{d}^{\mathscr{L}_l}\boldsymbol{\omega}}{\mathrm{d}t}\right)_{\mathscr{L}_0} &= \mathbb{I}_0 D(\boldsymbol{\beta})\mathbb{I}_1^{-1}\{\mathbf{N}_1 - [\boldsymbol{\omega}_1]_{\mathscr{L}_1} \times \mathbb{I}_1[\boldsymbol{\omega}_1]_{\mathscr{L}_1}\} - \mathbb{I}_0[\boldsymbol{\omega}_0]_{\mathscr{L}_0} \times [\boldsymbol{\omega}]_{\mathscr{L}_0} \\ &\quad - \{\mathbf{N}_0 - [\boldsymbol{\omega}_0]_{\mathscr{L}_0} \times \mathbb{I}_0[\boldsymbol{\omega}_0]_{\mathscr{L}_0}\}\end{aligned} \tag{9.20}$$

Finally, using Eq. (9.6) yields the equation for the relative attitude dynamics expressed using relative and $\mathscr{L}_0$-related angular velocities, i.e., without the deputy's angular velocities:

$$\begin{aligned}\mathbb{I}_0\left(\frac{\mathrm{d}^{\mathscr{L}_l}\boldsymbol{\omega}}{\mathrm{d}t}\right)_{\mathscr{L}_0} &= \mathbb{I}_0 D(\boldsymbol{\beta})\mathbb{I}_1^{-1}\Big\{\mathbf{N}_1 - D(\boldsymbol{\beta})^T([\boldsymbol{\omega}]_{\mathscr{L}_0} + [\boldsymbol{\omega}_0]_{\mathscr{L}_0}) \times \mathbb{I}_1 D(\boldsymbol{\beta})^T \\ &\quad \cdot ([\boldsymbol{\omega}]_{\mathscr{L}_0} + [\boldsymbol{\omega}_0]_{\mathscr{L}_0})\Big\} - \mathbb{I}_0[\boldsymbol{\omega}_0]_{\mathscr{L}_0} \times [\boldsymbol{\omega}]_{\mathscr{L}_0} \\ &\quad - \left\{\mathbf{N}_0 - [\boldsymbol{\omega}_0]_{\mathscr{L}_0} \times \mathbb{I}_0[\boldsymbol{\omega}_0]_{\mathscr{L}_0}\right\}\end{aligned} \tag{9.21}$$

Omitting the subscripts $\mathscr{L}_0$ and $\mathscr{L}_1$ and using the conventional notation $\dot{\boldsymbol{\omega}}$ to imply that $\boldsymbol{\omega}$ is both differentiated and expressed in $\mathscr{L}_0$ gives

$$\begin{aligned}\mathbb{I}_0\dot{\boldsymbol{\omega}} = \mathbb{I}_0 D\mathbb{I}_1^{-1}\Big[\mathbf{N}_1 - D^T([\boldsymbol{\omega}] + [\boldsymbol{\omega}_0]) \times \mathbb{I}_1 D^T([\boldsymbol{\omega}] + [\boldsymbol{\omega}_0])\Big] \\ -\mathbb{I}_0\boldsymbol{\omega}_0 \times \boldsymbol{\omega} - \left[\mathbf{N}_0 - \boldsymbol{\omega}_0 \times \mathbb{I}_0\boldsymbol{\omega}_0\right]\end{aligned} \tag{9.22}$$

Thus, the relative rotational kinematics and dynamics are described by Eqs. (9.7) and (9.22) for a seven-dimensional state vector $[\boldsymbol{\omega}^T, \boldsymbol{\beta}^T]^T$.

The complete relative motion is described by both the relative rotational and relative translational dynamics, which yields a system comprising a 15-element relative state vector $[\boldsymbol{\rho}^T, \dot{\boldsymbol{\rho}}^T, f, \dot{f}, \boldsymbol{\omega}^T, \boldsymbol{\beta}^T]^T$. The coupling between the rotational and translation dynamics arises because of either *external torques* (the most obvious example is the gravity gradient torque, which depends on altitude) or *internal coupling*, which is external-perturbations independent. The internal coupling stems from the fact that relative motion equations can be written for any point on the spacecraft, not necessarily the CM. Thus, an apparent translational motion of points on the deputy spacecraft (that do not coincide with the CM) will result from rotation of the deputy about its CM.

9.2 KINEMATICALLY-COUPLED RELATIVE SPACECRAFT MOTION MODEL

Consider two arbitrary feature points located on the chief and deputy spacecraft, as shown in Fig. 9.1. The spacecraft in this discussion are assumed to be rigid. Let P_0^j be a point on the chief. Then, $\mathbf{P}_0^j = [P_{x0}^j, P_{y0}^j, P_{z0}^j]^T$ is a vector directed from the origin of the coordinate system $\mathscr{L}_0$ to the point P_0^j. In the special case where $\mathbf{P}_0^j$ coincides with the chief's CM, $\mathbf{P}_0^0 = [0, 0, 0]^T$. Similarly, P_1^i is an arbitrary point on the deputy. Thus, $\mathbf{P}_1^i = [P_{x1}^i, P_{y1}^i, P_{z1}^i]^T$ is a vector directed from the origin of the coordinate system $\mathscr{L}_1$ to the point P_1^i, and $\mathbf{P}_1^0 = [0, 0, 0]^T$ is the vector description of the deputy's CM. Let $\boldsymbol{\rho}_{ij}$ denote the relative position vector between point j on the chief and point i on the deputy and $\boldsymbol{\rho}$ be, as before, the relative position vector between the CMs of the spacecraft. By observing Fig. 9.1, one can note that the following relationship holds:

$$\mathbf{P}_0^j + \boldsymbol{\rho}_{ij} = \boldsymbol{\rho} + \mathbf{P}_1^i \tag{9.23}$$

Thus,

$$\boldsymbol{\rho}_{ij} = \boldsymbol{\rho} + \mathbf{P}_1^i - \mathbf{P}_0^j \tag{9.24}$$

The first- and second-order time derivatives of $\boldsymbol{\rho}_{ij}$ are

$$\dot{\boldsymbol{\rho}}_{ij} = \dot{\boldsymbol{\rho}} + \dot{\mathbf{P}}_1^i - \dot{\mathbf{P}}_0^j \tag{9.25}$$

$$\ddot{\boldsymbol{\rho}}_{ij} = \ddot{\boldsymbol{\rho}} + \ddot{\mathbf{P}}_1^i - \ddot{\mathbf{P}}_0^j \tag{9.26}$$

where in frame $\mathscr{L}_0$,

$$\dot{\mathbf{P}}_0^j = \ddot{\mathbf{P}}_0^j = 0 \tag{9.27}$$

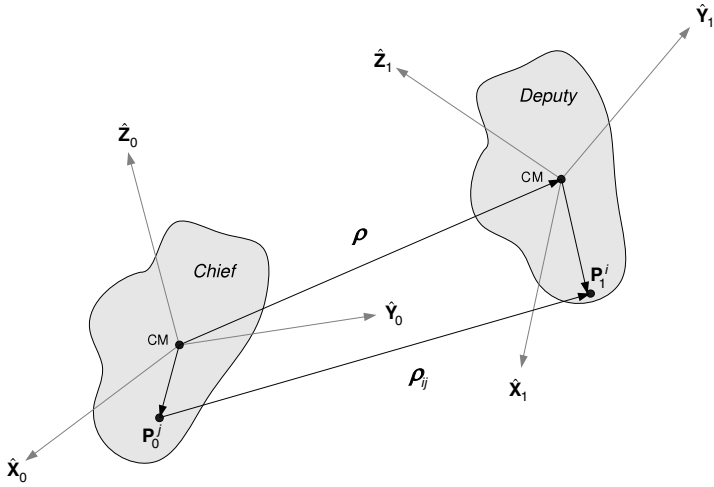

FIGURE 9.1 Two rigid-body spacecraft with body-fixed reference frames.

since the chief is assumed a rigid body. Calculating $\dot{\mathbf{P}}_1^i$ and $\ddot{\mathbf{P}}_1^i$ with respect to the rotating frame $\mathscr{L}_0$ results in

$$\left[\dot{\mathbf{P}}_1^i\right]_{\mathscr{L}_0} = \left[\dot{\mathbf{P}}_1^i\right]_{\mathscr{L}_1} + \boldsymbol{\omega} \times \mathbf{P}_1^i \tag{9.28}$$

$$\left[\ddot{\mathbf{P}}_1^i\right]_{\mathscr{L}_0} = \left[\ddot{\mathbf{P}}_1^i\right]_{\mathscr{L}_1} + 2\left\{\left[\boldsymbol{\omega} \times \dot{\mathbf{P}}_1^i\right]_{\mathscr{L}_1}\right\} + \dot{\boldsymbol{\omega}} \times \mathbf{P}_1^i + \boldsymbol{\omega} \times (\boldsymbol{\omega} \times \mathbf{P}_1^i) \tag{9.29}$$

Since the deputy is assumed a rigid body,

$$\left[\dot{\mathbf{P}}_1^i\right]_{\mathscr{L}_1} = \left[\ddot{\mathbf{P}}_1^i\right]_{\mathscr{L}_1} = 0$$

This leads us to the following equations:

$$\dot{\boldsymbol{\rho}}_{ij} = \dot{\boldsymbol{\rho}} + \boldsymbol{\omega} \times \mathbf{P}_1^i \tag{9.30}$$

$$\ddot{\boldsymbol{\rho}}_{ij} = \ddot{\boldsymbol{\rho}} + \dot{\boldsymbol{\omega}} \times \mathbf{P}_1^i + \boldsymbol{\omega} \times (\boldsymbol{\omega} \times \mathbf{P}_1^i) \tag{9.31}$$

Expressing the vectors using their components along frame $\mathscr{L}_0$, i.e. $\boldsymbol{\rho} = [x, y, z]^T$, $\boldsymbol{\rho}_{ij} = [x_{ij}, y_{ij}, z_{ij}]^T$, $\mathbf{P}_1^i = [P_{x_1}^i, P_{y_1}^i, P_{z_1}^i]^T$, $\mathbf{P}_0^j = [P_{x_0}^j, P_{y_0}^j, P_{z_0}^j]^T$, $\boldsymbol{\omega} = [\omega_x, \omega_y, \omega_z]^T$ and substituting into Eqs. (9.24), (9.30), (9.31) gives the following relationships for the relative position components:

$$x_{ij} = x + P_{x_1}^i - P_{x_0}^j \tag{9.32a}$$

$$y_{ij} = y + P_{y_1}^i - P_{y_0}^j \tag{9.32b}$$

$$z_{ij} = z + P_{z_1}^i - P_{z_0}^j \tag{9.32c}$$

the relative velocity components:

$$\dot{x}_{ij} = \dot{x} + \omega_y P^i_{z_1} - \omega_z P^i_{y_1} \tag{9.33a}$$

$$\dot{y}_{ij} = \dot{y} + \omega_z P^i_{x_1} - \omega_x P^i_{z_1} \tag{9.33b}$$

$$\dot{z}_{ij} = \dot{z} + \omega_x P^i_{y_1} - \omega_y P^i_{x_1} \tag{9.33c}$$

and the relative acceleration components:

$$\begin{aligned}\ddot{x}_{ij} = {} & \ddot{x} + \omega_y(\omega_x P^i_{y_1} - \omega_y P^i_{x_1}) - \omega_z(\omega_z P^i_{x_1} - \omega_x P^i_{z_1}) \\ & + \dot{\omega}_y P^i_{z_1} - \dot{\omega}_z P^i_{y_1}\end{aligned} \tag{9.34a}$$

$$\begin{aligned}\ddot{y}_{ij} = {} & \ddot{y} + \omega_z(\omega_y P^i_{z_1} - \omega_z P^i_{y_1}) - \omega_x(\omega_x P^i_{y_1} - \omega_y P^i_{x_1}) \\ & + \dot{\omega}_z P^i_{x_1} - \dot{\omega}_x P^i_{z_1}\end{aligned} \tag{9.34b}$$

$$\begin{aligned}\ddot{z}_{ij} = {} & \ddot{z} + \omega_x(\omega_z P^i_{z_1} - \omega_x P^i_{x_1}) - \omega_y(\omega_y P^i_{z_1} - \omega_z P^i_{y_1}) \\ & + \dot{\omega}_x P^i_{y_1} - \dot{\omega}_y P^i_{x_1}\end{aligned} \tag{9.34c}$$

The translational motion model describing the relative motion between the chief and deputy spacecraft CMs, i.e. a model for the case where $\mathbf{P}^i_1 = \mathbf{P}^j_0 = \mathbf{0}$, is usually written in the form

$$\ddot{\boldsymbol{\rho}} = \mathbf{g}_0(\boldsymbol{\rho}, r_0, \dot{f}_0, \ddot{f}_0)$$

as was shown in Chapter 4 and repeated in Eqs. (9.1). We have now obtained a more general model, in which

$$\ddot{\boldsymbol{\rho}}_{ij} = \mathbf{g}(\boldsymbol{\rho}_{ij}, r_0, \dot{f}_0, \ddot{f}_0, \boldsymbol{\omega}, \dot{\boldsymbol{\omega}}, \mathbf{P}^i_1, \mathbf{P}^j_0)$$

This model is obtained by substituting Eqs. (9.32)–(9.34) into Eqs. (9.1), to yield the following general description of the translational motion between any arbitrary points $\mathbf{P}^i$ and $\mathbf{P}^j$ in the absence of perturbing forces:

$$\begin{aligned}&\ddot{x}_{ij} - \left[\omega_y(\omega_x P^i_{y_1} - \omega_y P^i_{x_1}) + \omega_z(\omega_z P^i_{x_1} - \omega_x P^i_{z_1})\right] - \dot{\omega}_y P^i_{z_1} + \dot{\omega}_z P^i_{y_1} \\ &\quad - 2\dot{f}_0\left[\dot{y}_{ij} - (\omega_z P^i_{x_1} + \omega_x P^i_{z_1})\right] - \ddot{f}_0(y_{ij} - P^i_{y_1} + P^j_{y_0}) - \dot{f}_0^2(x_{ij} - P^i_{x_1} + P^j_{x_0}) \\ &\qquad = \frac{-\mu(r_0 + x_{ij} - P^i_{x_1} + P^j_{x_0})}{[(r_0 + x_{ij} - P^i_{x_1} + P^j_{x_0})^2 + (y_{ij} - P^i_{y_1} + P^j_{y_0})^2 + (z_{ij} - P^i_{z_1} + P^j_{z_0})^2]^{\frac{3}{2}}} \\ &\qquad\quad + \frac{\mu}{r_0^2}\end{aligned} \tag{9.35}$$

$$\begin{aligned}&\ddot{y}_{ij} - \left[\omega_z(\omega_y P^i_{z_1} - \omega_z P^i_{y_1}) + \omega_x(\omega_x P^i_{y_1} - \omega_y P^i_{x_1})\right] - \dot{\omega}_z P^i_{x_1} + \dot{\omega}_x P^i_{z_1} \\ &\quad + 2\dot{f}_0\left[\dot{x}_{ij} - (\omega_y P^i_{z_1} + \omega_z P^i_{y_1})\right] + \ddot{f}_0(x_{ij} - P^i_{x_1} - P^j_{x_0}) - \dot{f}_0^2(y_{ij} - P^i_{y_1} + P^j_{y_0}) \\ &\qquad = \frac{-\mu(y_{ij} - P^i_{y_1} + P^j_{y_0})}{[(r_0 + x_{ij} - P^i_{x_1} + P^j_{x_0})^2 + (y_{ij} - P^i_{y_1} + P^j_{y_0})^2 + (z_{ij} - P^i_{z_1} + P^j_{z_0})^2]^{\frac{3}{2}}}\end{aligned} \tag{9.36}$$

$$\ddot{z}_{ij} - \left[\omega_x(\omega_z P^i_{x_1} - \omega_x P^i_{z_1}) + \omega_y(\omega_y P^i_{z_1} - \omega_z P^i_{y_1})\right] - \dot{\omega}_x P^i_{y_1} + \dot{\omega}_y P^i_{x_1}$$
$$= \frac{-\mu(z_{ij} - P^i_{z_1} + P^j_{z_0})}{[(r_0 + x_{ij} - P^i_{x_1} + P^j_{x_0})^2 + (y_{ij} - P^i_{y_1} + P^j_{y_0})^2 + (z_{ij} - P^i_{z_1} + P^j_{z_0})^2]^{\frac{3}{2}}} \tag{9.37}$$

These equations are coupled to the rotational motion equations (9.7) and (9.22) through the components of the relative angular velocity vector, $\boldsymbol{\omega}$. Therefore, the six-DOF description of the rigid-body relative spacecraft motion is given by the following set of nonlinear coupled differential equations: Eqs. (9.35), (9.36), (9.37), Eqs. (9.7) and (9.22), together with the expressions for the true anomaly rate, given in Eq. (2.29).

An approximated set of translational equations of motion can be obtained using the same assumptions leading to the CW equations, i.e., a circular reference orbit and a small relative distance compared to the orbital radius. It should be noted that these assumptions lead to differential equations that will be linear with respect to the relative position, and nonlinear with respect to the components of the relative angular velocity vector. Thus, by applying the CW rationale on Eqs. (9.35), (9.36), and (9.37), the following approximate equations are obtained:

$$\dot{\mathbf{x}}_{tr} = A\mathbf{x}_{tr} + \mathbf{p} \tag{9.38}$$

where $\mathbf{x}_{tr} = [\boldsymbol{\rho}^T, \dot{\boldsymbol{\rho}}^T]^T$, $\dot{f}_0 = n = \text{const.}$,

$$A = \begin{bmatrix} 0 & 0 & 0 & 1 & 0 & 0 \\ 0 & 0 & 0 & 0 & 1 & 0 \\ 0 & 0 & 0 & 0 & 0 & 1 \\ 3n^2 & 0 & 0 & 0 & 2n & 0 \\ 0 & 0 & 0 & -2n & 0 & 0 \\ 0 & 0 & -n^2 & 0 & 0 & 0 \end{bmatrix} \tag{9.39}$$

and $\mathbf{p} = [0, 0, 0, p_1, p_2, p_3]^T$ is defined by

$$\begin{aligned} p_1 &\triangleq 3n^2(P^j_{x_0} - P^i_{x_1}) - 2n(\omega_z P^i_{x_1} - \omega_x P^i_{z_1}) \\ &\quad + \left[\omega_y(\omega_x P^i_{y_1} - \omega_y P^i_{x_1}) + \omega_z(\omega_z P^i_{x_1} - \omega_x P^i_{z_1})\right] + \dot{\omega}_y P^i_{z_1} - \dot{\omega}_z P^i_{y_1} \\ p_2 &\triangleq 2n(\omega_y P^i_{z_1} + \omega_z P^i_{y_1}) \\ &\quad + \left[\omega_z(\omega_y P^i_{z_1} - \omega_z P^i_{y_1}) + \omega_x(\omega_x P^i_{y_1} - \omega_y P^i_{x_1})\right] + \dot{\omega}_z P^i_{x_1} - \dot{\omega}_x P^i_{z_1} \\ p_3 &\triangleq n^2(P^i_{z_1} - P^j_{x_0}) + \left[\omega_x(\omega_z P^i_{x_1} - \omega_x P^i_{z_1}) + \omega_y(\omega_y P^i_{z_1} - \omega_z P^i_{y_1})\right] \\ &\quad + \dot{\omega}_x P^i_{y_1} - \dot{\omega}_y P^i_{x_1} \end{aligned} \tag{9.40}$$

These terms result from the coupling to the rotational dynamics, and can be treated as *kinematic perturbations*. However, these perturbations will always be present, regardless of the orbital altitude and external perturbations.

The kinematic coupling effect will be accentuated when the relative distances become small.

Example 9.1. *A chief is orbiting the Earth in an elliptic orbit with eccentricity* $e_0 = 0.05$*, semimajor axis* $a_0 = 7170$ *km and inclination* $i_0 = 15°$*. The argument of perigee of the chief satisfies* $\omega_0 = 340°$*, the right ascension of the ascending node is* $\Omega_0 = 0°$ *and the initial true anomaly is* $f_0(0) = 20°$*. The nonlinear coupled-motion model is used for simulating the relative distances between three feature points on the deputy,* $\mathbf{P}_1^i, i = 0, 1, 2$*, and the chief's CM,* $\mathbf{P}_0^0$*. These points are* $\mathbf{P}_0^0 = [0, 0, 0]^T$*,* $\mathbf{P}_1^0 = [0, 0, 0]^T$*,* $\mathbf{P}_1^1 = [1.5, 1.5, 0]^T$ m *and* $\mathbf{P}_1^2 = [-1.5, -1.5, 0]^T$ m*. The initial conditions are as follows:*

$$\begin{aligned} \boldsymbol{\rho}(0) &= [25, 25, 50]^T \text{ m}, \dot{\boldsymbol{\rho}}(0) = [0, -0.0555, 0]^T \text{ m/s} \\ \boldsymbol{\omega}(0) &= [0.1\dot{f}_0(0), 0.1\dot{f}_0(0), 2\dot{f}_0(0)]^T, \boldsymbol{\beta}(0) = [0, 0, 0, 1]^T \end{aligned} \tag{9.41}$$

where $\dot{f}_0(0) = 0.0656$ deg/s*. In addition,*

$$\mathbb{I}_0 = \mathbb{I}_1 = \mathbb{I} = \text{ diag}\{500, 550, 600\} \text{ kgm}^2$$

It can be readily verified that the given initial conditions were chosen to satisfy the energy matching condition (4.36):

$$\frac{1}{2}\left\{\left[\dot{x}(0) - \dot{f}_0(0)y(0) + \dot{r}_0(0)\right]^2 + \left[\dot{y}(0) + \dot{f}_0(0)(x(0) + r_0(0))\right]^2 + \dot{z}^2(0)\right\} - \frac{\mu}{\sqrt{[x(0) + r_0(0)]^2 + y^2(0) + z^2(0)}} = -\frac{\mu}{2a_0}$$

guaranteeing bounded relative motion between the spacecraft in the formation.

The initial conditions for the feature points on the deputy that do not coincide with the CM are calculated by applying Eqs. (9.24) and (9.30), which results in

$$\boldsymbol{\rho}_{10}(0) = [26.5, 26.5, 50]^T \text{ m}, \boldsymbol{\rho}_{20}(0) = [23.5, 23.5, 50]^T \text{ m} \tag{9.42}$$

The results of the formation flying simulation for a single orbital period of the chief are depicted by Figs. 9.2 and 9.3. Figure 9.2 shows the position components of the selected feature point on the deputy's body relative to the chief's CM, i.e. $\boldsymbol{\rho}_{10} = \boldsymbol{\rho} + \mathbf{P}_1^1 - \mathbf{P}_0^0$, $\boldsymbol{\rho}_{20} = \boldsymbol{\rho} + \mathbf{P}_1^2 - \mathbf{P}_0^0$ and $\boldsymbol{\rho}$ (the last vector represents the position of the deputy's CM relative to the chief's CM). Figure 9.3 shows the deviation in the relative position of the feature points due to the coupling effect. These deviations are defined as $\Delta\boldsymbol{\rho}_1 = \boldsymbol{\rho}_{10} - \boldsymbol{\rho}$ and $\Delta\boldsymbol{\rho}_2 = \boldsymbol{\rho}_{20} - \boldsymbol{\rho}$.

Figure 9.2 clearly demonstrates that the relative position between the chief's CM and the chosen feature points on the deputy depends upon the chosen points' location in the deputy's body frame. Moreover, Fig. 9.3 shows that the relative motion between the chief's CM and feature points on the deputy spacecraft that do not coincide with the deputy's CM exhibit harmonic oscillations whose frequency is determined by the relative angular velocity. The magnitude

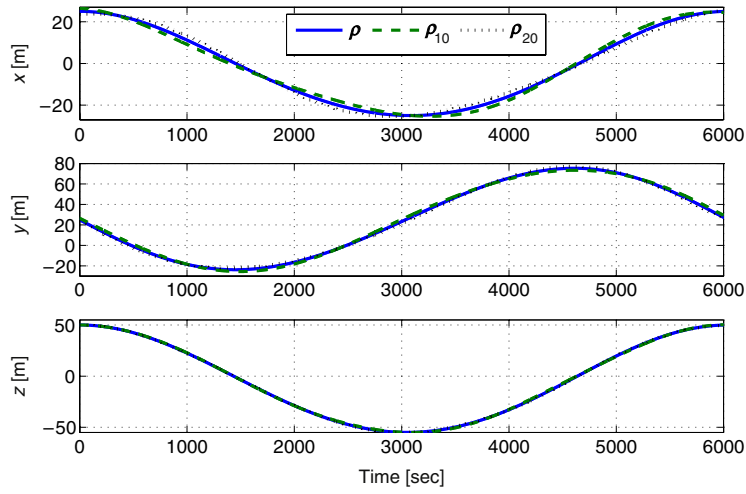

FIGURE 9.2 Time histories of the position components of several feature points on the deputy spacecraft relative to the chief's spacecraft center-of-mass.

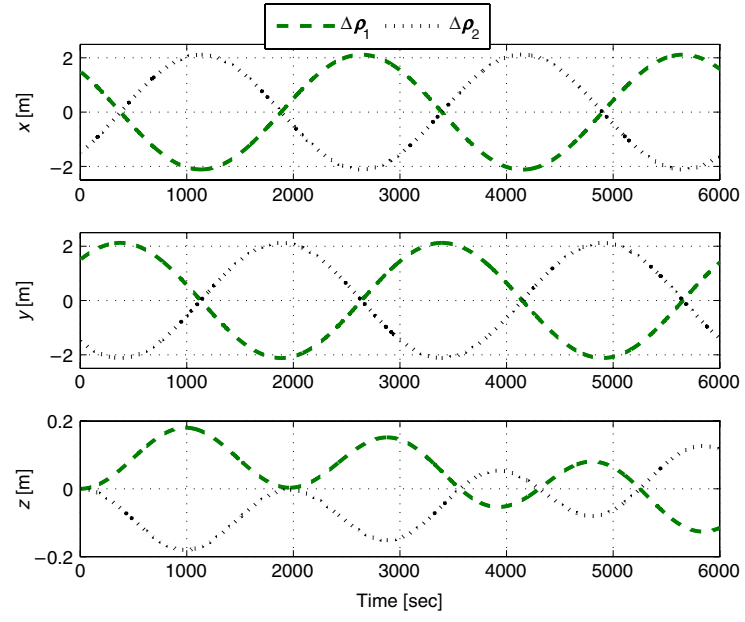

FIGURE 9.3 The time histories of the relative displacement components of points on the deputy spacecraft relative to the line joining the spacecraft centers of masses, showing that the kinematic coupling induces relative translational motion due to rotation.

of these oscillations depends on the location of the point in the deputy's body frame. Evidently, this result is different from standard six-DOF models, which

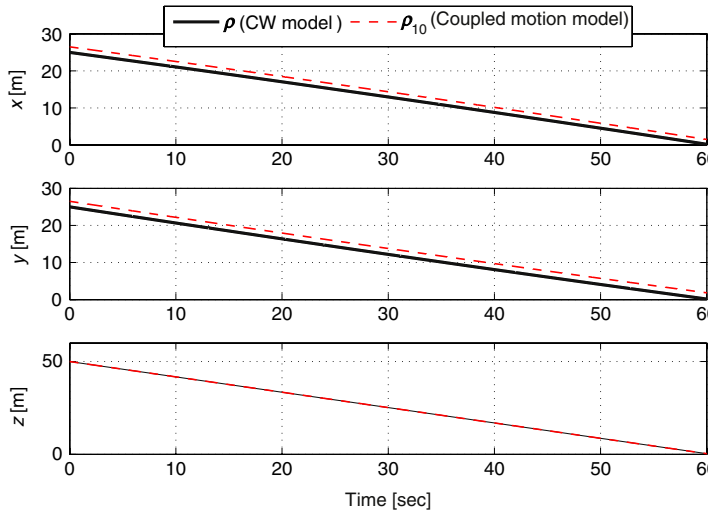

FIGURE 9.4 A comparison between the relative position components as modeled by the CW equations and the approximate model (9.38) for a rendezvous mission.

do not take the kinematic coupling into consideration, i.e., neglect the effect of the relative rotation on the relative translation.

Example 9.2. *A chief spacecraft is orbiting the Earth in a circular orbit with radius* $a_0 = 7170$ km. *The approximate model (9.38) is used to simulate the relative distance between two feature points,* $\mathbf{P}_1^i, i = 0, 1$ *on the deputy spacecraft and the chief spacecraft's CM,* $\mathbf{P}_0^0 = [0, 0, 0]^T$. *These points are selected as follows: The deputy's CM,* $\mathbf{P}_1^0 = [0, 0, 0]^T$, *and* $\mathbf{P}_1^1 = [1.5, 1.5, 0]^T$ m. *The initial conditions of the relative position and relative velocity were chosen so as to nullify the relative position* $\boldsymbol{\rho}$ *at the specified time* $t_1 = 0.01T = 60.42$ sec, *where* $T = 2\pi\sqrt{\frac{a_0^3}{\mu}} = 100.7$ min. *The resulting initial conditions are*

$$\boldsymbol{\rho}(0) = [25, 25, 50]^T \text{ m}, \dot{\boldsymbol{\rho}}(0) = [-0.3889, -0.4392, -0.8264]^T \text{ m/s} \quad (9.43)$$

$$\begin{aligned} \boldsymbol{\rho}_{10}(0) &= [26.5, 26.5, 50]^T \text{ m}, \\ \dot{\boldsymbol{\rho}}_{10}(0) &= [-0.392, -0.4361, -0.8264]^T \text{ m/s} \end{aligned} \quad (9.44)$$

and

$$\boldsymbol{\omega}(0) = [0.1n, 0.1n, 2n]^T \quad (9.45)$$

where $n = \sqrt{\frac{a_0^3}{\mu}} = 0.0010402$ rad/s.

The results of this rendezvous example are shown in Figs. 9.4 and 9.5. Figure 9.4 depicts the relative positions $\boldsymbol{\rho}$ and $\boldsymbol{\rho}_{10}$. Although the relative distance between the spacecrafts' CMs is decreasing to zero, the distance from

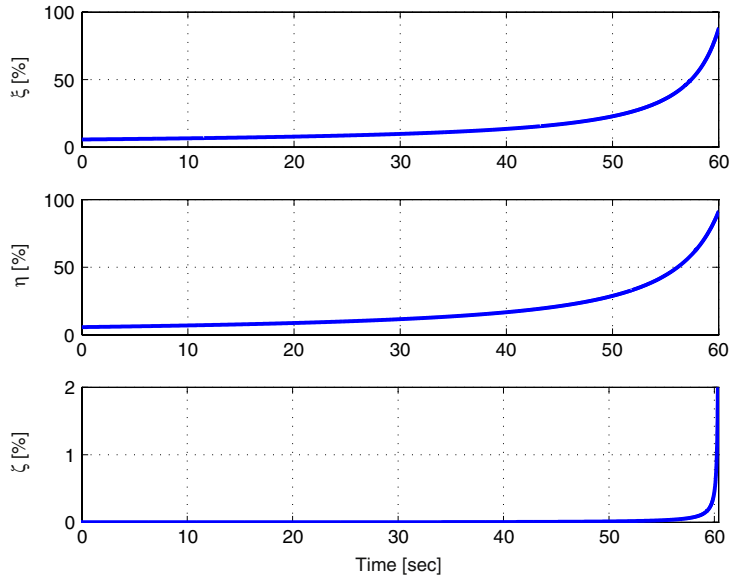

FIGURE 9.5 Although the CW model is widely used for the final approach phase of rendezvous missions, this figure shows that the effect of rotational-translation kinematic coupling impairs the validity of the CW model.

the chief's CM to the point $\mathbf{P}_1^1$ is not. Moreover, the normalized differences between model (9.38) and the CW model (Eqs. (5.4)–(5.6)), defined as

$$\xi = \frac{x_{10} - x}{x_{10}}, \eta = \frac{y_{10} - y}{y_{10}}, \zeta = \frac{z_{10} - z}{z_{10}} \tag{9.46}$$

reach 100% as $t \to t_f$, as can be seen in Fig. 9.5. Thus, this example clearly demonstrates that at the final approach phase of a rendezvous, the CW model will be invalid due to the kinematic coupling of rotation and translation.

SUMMARY

In this chapter, a kinematically coupled relative rotational and translational motion model, describing the six-degrees-of-freedom relative dynamics between two rigid-body spacecraft, was developed. This model generalizes the nonlinear relative translation models discussed in Chapter 4 to include trajectories of points that are not located on the spacecraft centers-of-mass (CMs). The relative motion of the non-CM points was illustrated by using two examples: A formation flying scenario and a rendezvous mission. The main observation is that neglecting the relative translation induced by the relative rotation can lead to considerable errors.

It was demonstrated that the points that are not located at the deputy's CM oscillate harmonically with respect to the chief's CM. This motion cannot be detected using traditional relative motion models. It was also shown that if the

kinematic coupling is neglected the CW equation can lead to considerable errors when applied to the modeling of rendezvous and docking.

Orbital perturbations discussed in Chapters 4 and 7 may induce differential dynamics that are more significant than the kinematic coupling effect. However, the latter effect is always present, even in short operation times (typical, e.g., to orbital rendezvous), where orbital perturbations are less dominant. In fact, the kinematic coupling effect does not depend on environmental perturbations and is an inherent part of the nominal relative motion equations. As such, it should be taken into account in the linearized relative-translation equations.